

## Gas-Phase Halonium Metathesis and Its Competitors. Skeletal Rearrangements of Cationic Adducts of Saturated Ketones

Philip S. Mayer,<sup>†</sup> Danielle Leblanc,<sup>‡</sup> and Thomas Hellman Morton\*<sup>†</sup>

Contribution from the Department of Chemistry, University of California, Riverside, California 92521-0403, and Laboratoire des Mécanismes Réactionnels, Ecole Polytechnique, 91128 Palaiseau, France

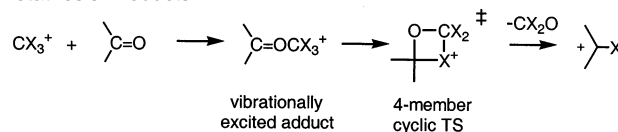
Received April 18, 2002

**Abstract:** The methyl cation and  $\text{CF}_3^+$  attack saturated, acyclic ketones to make vibrationally excited adduct ions. Despite their high internal energies and short lifetimes, these adducts undergo deep-seated rearrangements that parallel slower processes in solution. Observed pathways include alkene and alkane expulsions, in addition to (in the case of  $\text{CF}_3^+$ ) the precedented loss of  $\text{CF}_2\text{O} + \text{HF}$ . For the vast majority of ketones, the principal charged products are the  $\text{CF}_3^+$  adducts of lighter carbonyl compounds, ions that are not easily prepared by other avenues. Evidence for ion structures comes from collisionally activated unimolecular decomposition and bimolecular ion–molecule reactions. Typical examples are di-*n*-propyl and diisopropyl ketones (both of which produce  $\text{CH}_3\text{CH}=\text{OCF}_3^+$  as the principal ion–molecule reaction product) and pentamethylacetone (which produces  $(\text{CH}_3)_2\text{C}=\text{OCF}_3^+$  as virtually the sole ion–molecule reaction product). Isotopic labeling experiments account for mechanisms, and DFT calculations provide a qualitative explanation for the relative abundances of products from unimolecular decompositions of the chemically activated  $\text{CF}_3^+$  adduct ions that are initially formed.

Metathesis reactions of carbonyl compounds are relatively few in number, but they find many applications in organic chemistry. These reactions typically operate by forming a four-membered ring, which then splits to transfer the oxygen to a new atom. Most of the widely used examples (e.g., Peterson olefination or the Wittig and Lawesson reagents or the Tebbe, Schrock, and Petasis reactions<sup>1</sup>) require an oxygen acceptor that has low-lying *d*-orbitals (such as silicon, phosphorus, or a metal). In the gas phase, electron-deficient atoms such as boron can play a similar role (for instance, the metathesis of a boron-stabilized carbanion with carbon dioxide<sup>2</sup>).

A metathesis reagent needs to have an electrophilic center directly connected to a nucleophilic center (hence, the name *ylid* given to the Wittig reagent). The Lewis acidity of the electrophilic site and the Lewis basicity of the nucleophilic site must be carefully balanced. As one atom becomes less basic, the other can compensate by becoming more acidic. In the gas phase, even a methyl cation undergoes metathesis with acetone, as Scheme 1 depicts.<sup>3</sup> The electron-deficient carbon serves as the oxygen acceptor. It is such a strong Lewis acid that hydrogen ( $\text{X} = \text{H}$  or  $\text{D}$ ) can act as a nucleophile. Net transposition of  $\text{X}^+$

**Scheme 1.** Formation of Adduct Ions and Their Decomposition to Metathesis Products



for O creates an isopropyl cation, which represents about one-eighth of the total yield of ion–molecule reaction products.<sup>3</sup>

Overbalancing the acidity of the electron-deficient center causes competing reactions to occur (giving the bulk of the products when a methyl cation reacts with acetone<sup>3</sup>). This paper describes the skeletal rearrangements that ensue after  $\text{CH}_3^+$  and  $\text{CF}_3^+$  attach to carbonyl oxygens of homologues of acetone. To date, it has been an open question whether solution phase rearrangements, which can be monitored by NMR on a time scale of hours at room temperature, might also take place in chemically activated ions in less than a microsecond. The gas-phase experiments provide an affirmative answer, even for deep-seated, multistep isomerizations that require making and breaking more than one carbon–carbon bond.

Acid-mediated rearrangements of carbonyl compounds are a focus of current interest. Such isomerizations have been known for nearly a century,<sup>4</sup> but they have lately been found to play a role in natural product biosynthesis,<sup>5</sup> as well as in a variety of

\* E-mail: morton@citrus.ucr.edu.

<sup>†</sup> University of California.

<sup>‡</sup> Laboratoire des Mécanismes Réactionnels.

- (1) Fieser, M. et al., Eds. *Fieser & Fieser's Reagents for Organic Synthesis*; Wiley-Interscience: New York; pp 1967–2000.
- (2) Johlman, C. L.; Ijames, C. F.; Wilkins, C. L.; Morton, T. H. *J. Org. Chem.* **1983**, *48*, 2628–2629.
- (3) Smith, R. D.; Herold, D. A.; Elwood, T. A.; Futrell, J. H. *J. Am. Chem. Soc.* **1977**, *99*, 6042–6045.

(4) Wallach, O. *Justus Liebigs Ann. Chem.* **1907**, *356*, 227–249.

(5) Fedorov, S. N.; Radchenko, A. S.; Shubina, L. K.; Kalinovsky, A. I.; Gerasimenko, A. V.; Popov, D. Y.; Stonik, V. A. *J. Am. Chem. Soc.* **1977**, *99*, **2001**, *123*, 504–5.

catalysts that shift carbon–carbon bonds, ranging from superacids<sup>6</sup> to zeolites and clays<sup>7</sup> to enzymes.<sup>8</sup> For example, this kind of rearrangement plays a pivotal role in the conversion of a linear to a branched carbon skeleton in the nonmevalonate pathway for biosynthesis of terpenes.<sup>9</sup> Unlike protonated ketones, Lewis acid adducts in the gas phase display a delicate balance between metathesis and rearrangement. A tilt toward rearrangement signals that this reaction has a lower barrier, even if the final outcome requires a sequence of unimolecular isomerization steps.

Trifluoromethyl cation ( $\text{CF}_3^+$ ) presents a particularly good example for study. Its carbon is less electron deficient than that of  $\text{CH}_3^+$ , and fluorine is more nucleophilic than hydrogen. When  $\text{X} = \text{halogen}$ , the metathesis of  $\text{X}^+$  for O in Scheme 1 is very efficient. The isoelectronic transposition of  $\text{F}^+$  for O produces the 2-fluoroisopropyl cation (concomitant with  $\text{CF}_2\text{O}$  loss) as three-quarters of the total ion yield.<sup>10,11</sup> This metathesis is highly exothermic, so that the remainder of the resulting product ions come from HF loss after transposition. The 2-fluoroisopropyl cation extrudes HF via a four-center concerted elimination.<sup>12</sup>

Delocalization of lone pair electron density onto the cationic center stabilizes the monohalogenated ions formed by metathesis. The resonance structure representing this delocalization,  $>\text{C}=\text{X}^+$ , has the formal structure of a halonium ion.<sup>13</sup> Hence the transposition of  $\text{X}^+$  for oxygen is called a halonium metathesis when  $\text{X} = \text{halogen}$ . Rearrangements that move the positive charge elsewhere interfere with halonium metathesis. As will be discussed below, the contest between metathesis and rearrangement responds to the identity of the ketone as well as to that of the metathesis reagent ion.

## Experimental Section

Ketones were either purchased from commercial sources or else synthesized using conventional methods. Pentamethylacetone was prepared by addition of *tert*-butyllithium to isobutyraldehyde followed by oxidation with Jones reagent; 3,4-dimethyl-2-pentanone was prepared by reaction of 2,3-dimethylbutyric acid (Sapon Laboratories) with 2 mol of methylolithium.  $\alpha$ -Deuterated analogues (all >98 atom % D) were prepared by repetitive base-catalyzed exchange with  $\text{D}_2\text{O}$ .  $\beta$ -Deuterated analogues were prepared by base-promoted methylation with  $\text{CD}_3\text{I}$  (Aldrich,  $\geq 99.5$  atom % D) in sealed tubes following a procedure published a century ago.<sup>14</sup> Contrary to that original report, these alkylations gave product mixtures whose chemical ionization (CI) mass spectra (using both  $\text{CF}_4$  and  $\text{CH}_4$  reagent gases) were examined using GC/MS on an HP5989A quadrupole mass spectrometer with  $10^{-4}$  Torr reagent gas pressure in the ion source and sample introduction via a 15 m  $\times$  0.25 mm DB-WAX capillary column in series with a 30 m  $\times$  0.25 mm DB-5HT column mounted in an HP5890 gas chromat-

graph. The combination of these two GC columns was required in order to effect clean separation of the isomer mixtures. The  $\text{CF}_4$  CI of compound **11a**, which was prepared by adding isopropyllithium to  $^{13}\text{CO}_2$  (CIL, 99% isotopic purity) followed by conversion of the carboxylic acid to its acid chloride and subsequent reaction with excess isopropyllithium, was also examined by GC/MS.

$\text{CF}_4$  CI spectra (using 70 eV electron ionization) of pure ketones were recorded on a VG ZAB-2F reverse geometry (B–E) two-sector instrument, with  $10^{-4}$  Torr  $\text{CF}_4$  pressure in the ion source. Reported ion abundances are the averages of three independent determinations. Exact mass and collisionally activated decomposition (CAD) measurements were performed on this instrument using conventional techniques. Some ions result from both electron ionization and CI, and it was difficult in most cases to assess the CI contribution. Therefore, an FT-ICR spectrometer was used to study the reactions of selected ketones with  $\text{CF}_3^+$  ions.

Ion–molecule reactions were studied in a Bruker CMS 47-X FT-ICR spectrometer equipped with an external ion source.  $\text{CF}_3^+$  ( $m/z$  69) ions formed by electron ionization on 2-iodoperfluoropropane (Aldrich) in the external ion source were transferred to the ICR cell and trapped there. Desired reactant ions were isolated in the cell by a series of rf ejection pulses to remove all other ions. Once isolated, these ions were allowed to relax by collisions with argon bath gas at  $(2-3) \times 10^{-7}$  mbar and then permitted to react with neutrals ( $2 \times 10^{-8}$  mbar static pressure) in the presence of argon. Collisionally activated decompositions of selected ions were performed using sustained off-resonance irradiation (SORI) CAD.

DFT calculations were performed using GAUSSIAN 98. Computations were performed at the B3LYP/6-31G\*\* level, unless otherwise specified. Zero point energy differences are based on unscaled harmonic normal-mode frequency calculations. Basis set superposition error (BSSE) was estimated using the counterpoise method. All stable geometries were confirmed using normal mode calculations, and all transition states were found to exhibit one negative force constant, whose motion corresponded to the expected reaction coordinate (as shown by animation using GaussView).

## Results

The experiments described below give the surprising result that multistep rearrangements operate in preference to metathesis. Because addition of  $\text{CF}_3^+$  to carbonyl oxygen produces an adduct ion with 125–165 kJ mol<sup>-1</sup> in excess of the barrier to metathesis,<sup>15</sup> it was not anticipated that complicated skeletal rearrangements would compete so effectively with the simple transposition of  $\text{F}^+$  for O. This work sought, as its original objective, to discover how the overall loss of  $\text{CF}_2\text{O} + \text{HF}$  takes place, so as to maximize the yield of metathesis ions. It was prompted by the observation that  $\text{CF}_4$  CI of 2-butanone in a sector mass spectrometer gives about 3 times more metathesis ion (relative to overall loss of  $\text{CF}_2\text{O} + \text{HF}$ ) than has been reported in the ICR spectrometer.<sup>11</sup> Upon closer inspection, it was discovered that 2-butanone also exhibits a reaction (addition of  $\text{CF}_3^+$  followed by ethylene loss) that had not been previously described. This type of reaction comes to dominate the chemistry of larger ketones.

Electron ionization of  $\text{CF}_4$  generates  $\text{CF}_3^+$  ions in high yield.<sup>15</sup> Chemical ionization of ketones and aldehydes with  $\text{CF}_4$  reagent gas offers a straightforward way to create gaseous fluorinated cations that are otherwise hard to make. However, as the carbonyl compound gets larger, avenues for HF expulsion from the halonium metathesis ions become prevalent, and overall loss

- (6) Olah, G. A.; Surya Prakash, G. K.; Mathew, T.; Marinez, E. R. *Angew. Chem., Int. Ed.* **2000**, *39*, 2547–2548.  
 (7) Elings, J. A.; Lempers, H. E. B.; Sheldon, R. A. *Eur. J. Org. Chem.* **2000**, 1905–1911.  
 (8) Eisenreich, W.; Schwarz, M.; Cartayrade, A.; Arigoni, D.; Zenk, M. H.; Bacher, A. *Chem. Biol.* **1998**, *5*, R221–R233.  
 (9) Koppisch, A. T.; Fox, D. T.; Blagg, B. S. J.; Poulter, C. D. *Biochemistry* **2002**, *41*, 236–243.  
 (10) Eyler, J. R.; Ausloos, P.; Lias, S. G. *J. Am. Chem. Soc.* **1974**, *96*, 3673–3675.  
 (11) Ausloos, P.; Lias, S.G.; Eyler, J. R. *Int. J. Mass Spectrom. Ion Processes* **1975**, *18*, 261–271.  
 (12) (a) Redman, E. W.; Johri, K. K.; Lee, R. W. K.; Morton, T. H. *J. Am. Chem. Soc.* **1984**, *106*, 4639–4640. (b) Redman, E. W.; Johri, K. K.; Morton, T. H. *J. Am. Chem. Soc.* **1985**, *107*, 780–784. (c) Stams, D. A.; Johri, K. K.; Morton, T. H. *J. Am. Chem. Soc.* **1988**, *110*, 699–706. (d) Shaler, T. A.; Morton, T. H. *J. Am. Chem. Soc.* **1991**, *113*, 6771–6779.  
 (13) Stams, D. A.; Thomas, T. D.; MacLaren, D.; Ji, D.; Morton, T. H. *J. Am. Chem. Soc.* **1990**, *112*, 1427–1434.  
 (14) Nef, J. U. *Justus Liebigs Ann. Chem.* **1900**, *310*, 316–335.

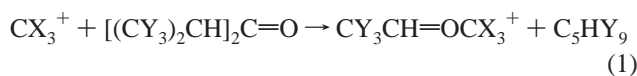
- (15) Nguyen, V.; Mayer, P. S.; Morton, T. H. *J. Org. Chem.* **2000**, *65*, 8032–8040.

of  $\text{CF}_2\text{O} + \text{HF}$  overshadows metathesis.<sup>11,15</sup> We recently surveyed the reactions of  $\text{CF}_3^+$  with unsaturated carbonyl compounds, to assess the scope and limitations of halonium metathesis for creating fluorinated allylic cations.<sup>16</sup> This study revealed a set of rearrangements leading to HF loss, even when the carbon skeleton would have been expected to preclude that elimination. The present paper describes a systematic examination of the reactions of  $\text{CF}_3^+$  with all the saturated, acyclic  $\text{C}_5$ ,  $\text{C}_6$ , and  $\text{C}_7$  ketones, which uses a variety of mass spectrometric techniques to explore the pathways that compete with metathesis.

As it happens, only one of the two dozen  $\text{C}_5$ – $\text{C}_7$  ketones (namely pinacolone) exhibits a detectable ion corresponding to halonium metathesis in its  $\text{CF}_4$  CI spectrum (about 0.05 the intensity of the peak corresponding to loss of  $\text{CF}_2\text{O} + \text{HF}$ ). Moreover, that ketone is the only one (besides isopropyl methyl ketone<sup>11</sup>) for which loss of  $\text{CF}_2\text{O} + \text{HF}$  dominates. While the goal of better understanding how HF is lost was achieved, an even more interesting outcome was found. In all the other ketones (with the exception of neopentyl methyl ketone), the expulsion of neutral hydrocarbons prevails, producing ions corresponding to trifluoromethylated aldehyde and ketones. Such species are also difficult to prepare in any other way.<sup>15,16</sup> This paper probes the mechanisms by which that novel category of fluorinated ions arises and dissects various pathways by which they form.

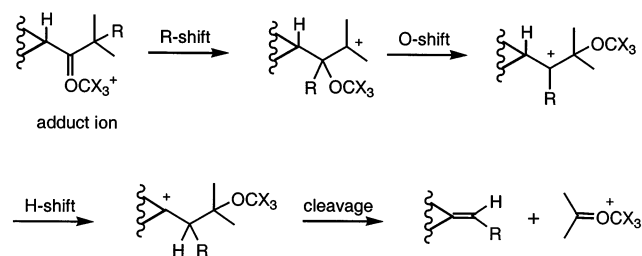
Many gaseous compounds react with  $\text{CF}_3^+$  and have been studied by ion cyclotron resonance<sup>10,11,17</sup> and ion-beam<sup>18</sup> techniques, as well as by use of  $\text{CF}_4$  as a CI reagent gas in a sector field mass spectrometer.<sup>15</sup> Adducts of  $\text{CF}_3^+$  with simple ketones are well-known to expel  $\text{CF}_2\text{O} + \text{HF}$ .<sup>10,11,15</sup> None of the previous reports discusses rearrangement/hydrocarbon expulsion, which (as described below) constitutes the major pathway for the vast majority of saturated, acyclic  $\text{C}_5$ – $\text{C}_7$  ketones and shows interesting parallels with the chemistry of  $\text{TMS}^+$  adducts.<sup>19,20</sup>

**Methyl Cation Reactions with  $\text{C}_7\text{H}_{14}\text{O}$ .** A representative example illustrates the type of reaction that dominates the chemistry of Lewis superacidic cations with acyclic  $\text{C}_5$ – $\text{C}_7$  ketones. The ion–molecule reactions of diisopropyl ketone with a methyl cation include the outcome summarized in eq 1. In the FT-ICR spectrometer,  $\text{CD}_3^+$  reacts with diisopropyl ketone ( $\text{C}_7\text{H}_{14}\text{O}$ ) to give (among other products) an ion with the formula  $\text{C}_3\text{H}_4\text{D}_3\text{O}^+$  ( $m/z$  62). The methylated acetaldehyde ion, as drawn in eq 1 ( $\text{X} = \text{D}$ ,  $\text{Y} = \text{H}$ ), would seem the most plausible structure.



Several features of this reaction warrant comment. Methane chemical ionization of labeled diisopropyl ketone ( $\text{X} = \text{H}$ ,  $\text{Y}$

**Scheme 2.** Oxygen Transposition Pathway to Rearrangement Products



= D) in the source of a quadrupole mass spectrometer gives an ion having the same mass. It seems reasonable to conclude that the deuterated and undeuterated methyl groups are transposed in the ion from methane CI, relative to the FT-ICR experiment outlined in the previous paragraph. Similarly, methane CI of  $(\text{CD}_3)_3\text{CCOCH}_2\text{CD}_3$  also yields an ion having the same mass (and, one presumes, the same structure). Deep-seated skeletal rearrangements must be occurring prior to dissociation. The expelled neutrals contain the elements of pentene, but neither diisopropyl ketone nor *tert*-butyl ethyl ketone has the connectivity needed to extrude a  $\text{C}_5$ -unit or a  $\text{C}_3$ -unit plus a  $\text{C}_2$ -unit. An analogous extrusion represents far and away the most intense metastable ion decomposition of the trimethylsilyl ( $\text{TMS}^+$ ) adduct of diisopropyl ketone,  $i\text{Pr}_2\text{C}=\text{OSiMe}_3^+ \rightarrow \text{MeCH}=\text{OSiMe}_3^+$ .<sup>20</sup>

No product ion corresponding to  $(\text{CH}_3)_2\text{C}=\text{OCD}_3^+$  ( $m/z$  76) is detected in the FT-ICR spectrometer when diisopropyl ketone reacts with  $\text{CD}_3^+$ . That result parallels the reported decomposition of the  $\text{TMS}^+$  adduct, where the most intense peak ( $\text{MeCH}=\text{OSiMe}_3^+$ ) is more abundant than any other fragment ion by a factor of  $>15$ . In both cases, failure to observe the more massive ion is surprising because, as Scheme 2 illustrates, a plausible pathway exists for  $\text{R}=\text{H}$  that would have given an outcome that is considerably more thermochemically favorable.

**Trifluoromethyl Cation Reactions with Ketones.** The same sort of reaction as that drawn in eq 1 occurs between  $\text{CF}_3^+$  and diisopropyl ketone ( $\text{X} = \text{F}$ ,  $\text{Y} = \text{H}$ ). Here, the product ion structure can be identified by its collisionally activated decomposition (CAD), since it expels  $\text{CF}_2\text{O}$  (as  $\text{CF}_3^+$ -adducts of simple carbonyl compounds are well-known to do<sup>10,11,16</sup>). Because CAD often permits structural assignments for fluorine-containing ions, a detailed investigation of the reaction of  $\text{CF}_3^+$  with all the saturated, acyclic  $\text{C}_5$ – $\text{C}_7$  ketones and several of their isotopically substituted analogues has been pursued.

Metathesis of  $\text{F}^+$  for  $\text{O}$  almost certainly occurs via a four-membered cyclic transition state, for which extensive DFT calculations have been reported.<sup>15</sup> Starting from the  $\text{CF}_3^+$ -adduct, we calculated activation barriers to be on the order of  $125$ – $160$   $\text{kJ mol}^{-1}$  for simple saturated carbonyl compounds. These barriers are much lower than the exothermicity of the initial attachment of  $\text{CF}_3^+$  to oxygen, and the resulting halonium metathesis ions have enough energy to lose HF subsequently. This precedent establishes a benchmark against which competing reactions (such as eq 1) can be compared.

Alkene expulsion predominates in the reactions of  $\text{CF}_3^+$  with acyclic ketones having five or more carbons. Table 1 summarizes the proportions of the major ionic products from  $\text{CF}_4$

(16) Leblanc, D.; Kong, J.; Mayer, P. S.; Morton, T. H. *Int. J. Mass Spectrom.* **2002**, *219*, 525–535.

(17) (a) Grandinetti, F.; Occhiucci, G.; Crestoni, M. E.; Fornarini, S.; Speranza, M. *Int. J. Mass Spectrom. Ion Processes* **1993**, *127*, 123–136. (b) Grandinetti, F.; Occhiucci, G.; Crestoni, M. E.; Fornarini, S.; Speranza, M. *Int. J. Mass Spectrom. Ion Processes* **1993**, *127*, 137–145. (c) Grandinetti, F.; Crestoni, M. E.; Fornarini, S.; Speranza, M. *Int. J. Mass Spectrom. Ion Processes* **1993**, *130*, 207–222.

(18) Tsuji, M.; Aizawa, M.; Nishimura, Y. *Bull. Chem. Soc. Jpn.* **1996**, *69*, 1055–1063.

(19) Bosma, N. L.; Harrison, A. G. *Rapid Commun. Mass Spectrom.* **1994**, *8*, 886–890.

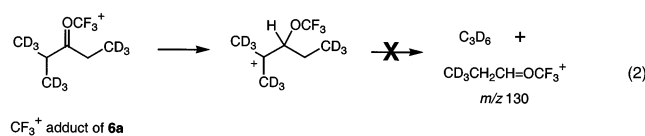
(20) Leblanc, D.; Kong, J.; Mayer, P. S.; Morton, T. H. *Int. J. Mass Spectrom.* **2002**, *217*, 257–271.



**Table 2.** Product Ion Distributions (Percent of Total) from CF<sub>4</sub> Chemical Ionization of Deuterated Isopropyl and *tert*-Butyl Ethyl Ketones<sup>a</sup>

	<i>m/z</i> 113	<i>m/z</i> 116	<i>m/z</i> 127	<i>m/z</i> 130	<i>m/z</i> 133
<b>6a</b> (CD <sub>3</sub> ) <sub>2</sub> CHCOCH <sub>2</sub> CD <sub>3</sub>	<0.5	72.8 (5.2)	<0.5	<0.5	18.0 (2.3)
<b>6b</b> CH <sub>3</sub> (CD <sub>3</sub> )CHCOCH <sub>2</sub> CH <sub>3</sub>	44.6 (1.1)	31.9 (0.8)	1.8 (0.3)	12.1 (0.7)	<0.5
<b>6c</b> (CH <sub>3</sub> ) <sub>2</sub> CHCOCH <sub>2</sub> CD <sub>3</sub>	61.0 (1.0)	13.6 (0.3)	10.7 (0.2)	3.6 (0.1)	<0.5
<b>17a</b> CH <sub>3</sub> (CD <sub>3</sub> ) <sub>2</sub> CCOCH <sub>2</sub> CH <sub>3</sub>	15.9 (4.2)	7.9 (2.6)	<0.5	47.2 (3.8)	22.7 (1.6)
<b>17b</b> CD <sub>3</sub> (CH <sub>3</sub> ) <sub>2</sub> CCOCH <sub>2</sub> CD <sub>3</sub>	6.2 (0.3)	13.2 (0.5)	23.3 (0.1)	47.7 (0.6)	1.0 (0.1)
<b>17c</b> CD <sub>3</sub> (CH <sub>3</sub> ) <sub>2</sub> CCOCH <sub>2</sub> CH <sub>3</sub>	14.5 (1.6)	3.6 (0.5)	24.9 (1.0)	47.2 (1.3)	<0.5

<sup>a</sup> Standard deviations given in parentheses.

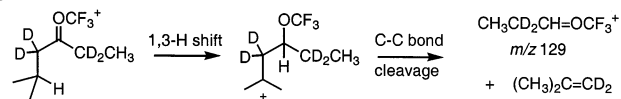
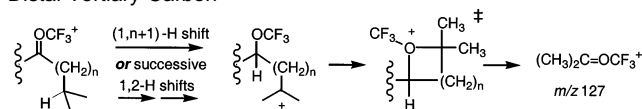


eq 2). As Table 2 summarizes, a contrary result obtains that *m/z* 133 is produced, demonstrating that the ionic product must be (CD<sub>3</sub>)<sub>2</sub>C=OCF<sub>3</sub><sup>+</sup>. It seems reasonable to conclude that an oxygen transposition mechanism, exemplified by Scheme 2, produces this ion.

It is worthwhile noting that little or no isotope effect appears to result from the substitutions of CD<sub>3</sub> for CH<sub>3</sub> in Table 2. The observation of CD<sub>3</sub>CH=OCF<sub>3</sub><sup>+</sup> and CH<sub>3</sub>CH=OCF<sub>3</sub><sup>+</sup> for both of the β-*d*<sub>3</sub> analogues of isopropyl ethyl ketone, **6b** and **c**, in Table 2 shows that all three methyl groups participate in forming the most abundant product ion. However, the proportions indicate that the two isopropyl methyls participate to a greater extent than does the methyl of the ethyl group. Nevertheless, the abundance ratio of MeCH=OCF<sub>3</sub><sup>+</sup> to Me<sub>2</sub>C=OCF<sub>3</sub><sup>+</sup> (including all of the isotopomers that are formed) remains equal to 5 (within experimental uncertainty) for all three of the deuterated analogues. Moreover, if we suppose there to be no isotope effect, the proportions of *m/z* 113 and *m/z* 116 observed from **6c** would predict (on a naïve statistical basis) that one should see proportions of (13.6 + 61/2):61/2 = 44:30.5 for **6b**, within experimental uncertainty of the actual proportions observed.

Ketone **17** differs from **6** in that its principal product ion (*m/z* 127) is Me<sub>2</sub>C=OCF<sub>3</sub><sup>+</sup>. A half-dozen deuterated analogues were studied, of which the results for three (**17a–c**) are summarized in Table 2. The β,β'-*d*<sub>12</sub> analogue (CD<sub>3</sub>)<sub>3</sub>CCOCH<sub>2</sub>CD<sub>3</sub> (not tabulated) gives only (CD<sub>3</sub>)<sub>2</sub>C=OCF<sub>3</sub><sup>+</sup> and CD<sub>3</sub>CH=OCF<sub>3</sub><sup>+</sup>. When only the ethyl group is β-deuterated, the (CH<sub>3</sub>)<sub>2</sub>C=OCF<sub>3</sub><sup>+</sup> ion exceeds its deuterated analogues by a factor of ≥40:1. As Table 2 summarizes, the β-*d*<sub>6</sub> analogue **17a** gives a 2:1 mixture of CH<sub>3</sub>(CD<sub>3</sub>)C=OCF<sub>3</sub><sup>+</sup> and (CD<sub>3</sub>)<sub>2</sub>C=OCF<sub>3</sub><sup>+</sup>, while the β-*d*<sub>6</sub> analogue **17b** gives a 2:1 mixture of CH<sub>3</sub>(CD<sub>3</sub>)C=OCF<sub>3</sub><sup>+</sup> and (CH<sub>3</sub>)<sub>2</sub>C=OCF<sub>3</sub><sup>+</sup>. The β-*d*<sub>3</sub> analogue **17c** gives the same proportions (within experimental uncertainty) of CH<sub>3</sub>(CD<sub>3</sub>)C=OCF<sub>3</sub><sup>+</sup> and (CH<sub>3</sub>)<sub>2</sub>C=OCF<sub>3</sub><sup>+</sup> as does **17b**. These measured ion abundance ratios are so close to the statistical proportions expected from Scheme 2 that the deuterium isotope effect must be negligible.

Formation of MeCH=OCF<sub>3</sub><sup>+</sup> from **17a–c** behaves as though the methyl comes from the ethyl group roughly one-half of the time and from the *tert*-butyl the other half, again with a negligible isotope effect. The complementarily labeled β-*d*<sub>6</sub> compounds **17a** and **b** give 2:1 and 1:2 intensity ratios of *m/z* 113 to *m/z* 116, respectively. Furthermore, CF<sub>4</sub> chemical ionization of (CH<sub>3</sub>)<sub>3</sub>CCOCD<sub>2</sub>CD<sub>3</sub> produces a 1.2:1 ratio of CD<sub>3</sub>CD=OCF<sub>3</sub><sup>+</sup> to CH<sub>3</sub>CD=OCF<sub>3</sub><sup>+</sup> (with virtually no ions

**Scheme 4.** Products from a 1,3-Hydrogen Shift in the Adduct Ion of **22****Scheme 5.** Hydrogen Shifts Leading to Oxygen Transposition to a Distal Tertiary Carbon

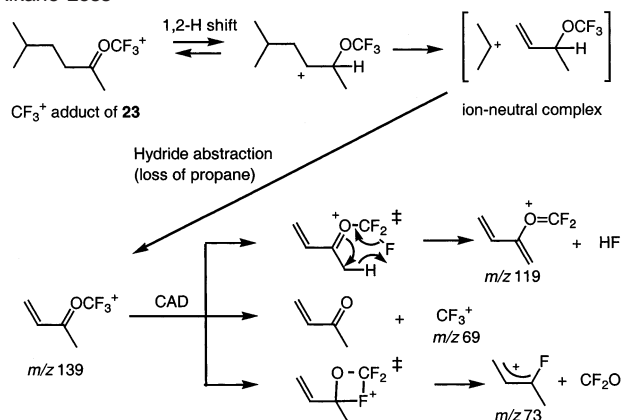
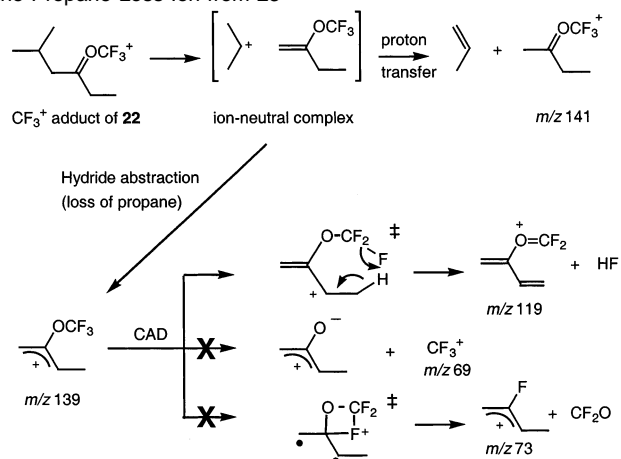
having H on the aldehydic carbon), while (CH<sub>3</sub>)<sub>3</sub>CCOCH<sub>2</sub>CD<sub>3</sub> produces CD<sub>3</sub>CH=OCF<sub>3</sub><sup>+</sup> to CH<sub>3</sub>CH=OCF<sub>3</sub><sup>+</sup> in virtually the same ratio.

In contrast to the α-branched ketones, the CF<sub>3</sub><sup>+</sup> adduct of isobutyl ethyl ketone (**22**) produces both EtCH=OCF<sub>3</sub><sup>+</sup> and Me<sub>2</sub>C=OCF<sub>3</sub><sup>+</sup>, as revealed by examination of the α,α'-perdeuterated analogue *i*PrCD<sub>2</sub>COCD<sub>2</sub>CH<sub>3</sub>. CF<sub>4</sub> chemical ionization of **22-α,α'-d**<sub>4</sub> produces *m/z* 127, *m/z* 129, and *m/z* 130 in a 0.25:0.90:1 ratio. The *m/z* 129 ion undoubtedly arises via a 1,3-hydrogen shift (which may occur in concert with C–C bond cleavage), as Scheme 4 depicts, to form CH<sub>3</sub>CD<sub>2</sub>CH=OCF<sub>3</sub><sup>+</sup>. The analogous pathway has precedent in the metastable ion decomposition of the (CH<sub>3</sub>)<sub>3</sub>Si<sup>+</sup> adduct of isobutyl methyl ketone.<sup>20</sup> A 1,3-oxygen migration to the intermediate tertiary cation, as portrayed in Scheme 5 for *n* = 1, accounts for the unlabeled ion from the deuterated precursor, which surely has the structure (CH<sub>3</sub>)<sub>2</sub>C=OCF<sub>3</sub><sup>+</sup>. More distal shifts also appear to be possible: CF<sub>4</sub> chemical ionization of α,α'-perdeuterated 5-methyl-2-hexanone (**23-α-d**<sub>5</sub>) yields *m/z* 127 as the principal C<sub>4</sub> product, suggesting that 1,4-migration of CF<sub>3</sub>O takes place, as shown in Scheme 5 for *n* = 2.

A variety of structures are possible for the C<sub>4</sub>H<sub>6</sub>OCF<sub>3</sub><sup>+</sup> product ion (*m/z* 139), which corresponds to loss of propane from the CF<sub>3</sub><sup>+</sup> adducts of the heptanones. Alkane loss is typically a hallmark of intermediate ion–neutral complexes,<sup>22</sup> often taking place via hydride abstraction. CF<sub>4</sub> CI of the C<sub>7</sub> ketones leads to small but measurable amounts of propane loss and even lower levels of butane (or isobutane) loss. While these represent minor pathways, structures can be deduced for the resulting ions. Schemes 6 and 7 depict sequences of steps by which the CF<sub>3</sub><sup>+</sup> adducts of 5-methyl-2-hexanone (**23**) and 5-methyl-3-hexanone (**22**) can lose propane.

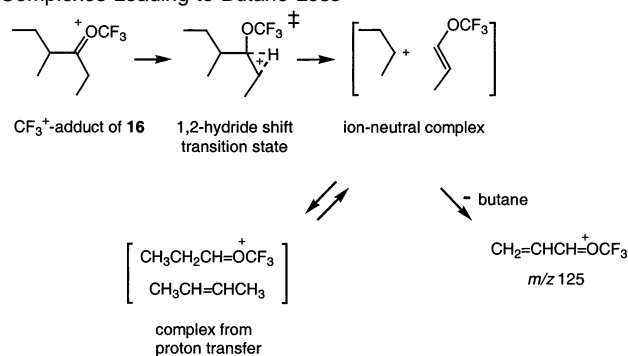
In Scheme 6, the initially formed CF<sub>3</sub><sup>+</sup> adduct of 5-methyl-2-hexanone isomerizes via a 1,2-hydride shift to form a secondary cation, which can easily cleave a bond to give anion–neutral complex between isopropyl cation and 2-trifluoro-

(22) (a) Audier, H. E.; Dahhani, F.; Milliet, A.; Kuck, D. *J. Chem. Soc., Chem. Commun.* **1997**, 429–430. (b) McAadoo, D. J.; Bowen, R. D. *Eur. Mass Spectrom.* **1999**, *5*, 389–409.

**Scheme 6.** An Ion–Neutral Complex as an Intermediate for Alkane Loss**Scheme 7.** Differentiation of the Propane Loss Ion from **22** from the Propane Loss Ion from **23**

methoxy-3-butene, as drawn. DFT calculations show that the electron-withdrawing effect of the trifluoromethoxy group makes the proton affinity of 2-trifluoromethoxy-3-butene only 39 kJ mol<sup>-1</sup> greater than that of propene. Proton transfer yields the *m/z* 141 ion. But, that is not as favorable as hydride abstraction to expel propane and yield the CF<sub>3</sub><sup>+</sup> adduct of methyl vinyl ketone (*m/z* 139), a pathway that is 134 kJ mol<sup>-1</sup> more exothermic than proton transfer. Confirmation of the *m/z* 139 ion structure comes from its CAD fragmentation pattern. In addition to H<sub>2</sub> loss and HF loss (the most intense ions in the CAD spectrum), prominent peaks come from expulsion of the neutral ketone to give CF<sub>3</sub><sup>+</sup> (*m/z* 69) and expulsion of CF<sub>2</sub>O to give a fluoroallylic ion (*m/z* 73).

The ion formed by expulsion of propane from the CF<sub>3</sub><sup>+</sup> adduct of 5-methyl-3-hexanone (**22**), portrayed in Scheme 7, behaves differently. A simple bond cleavage of the adduct ion can make an ion–neutral complex containing the isopropyl cation, without the necessity of a prior rearrangement. Hence, complex-mediated pathways operate to a greater extent in the CF<sub>4</sub> CI of **22** than for any of the other ketones under examination. The neutral partner from the simple cleavage has the structure of 2-trifluoromethoxy-1-butene, whose proton affinity is much greater than that of propene. As a consequence, proton transfer (which expels propene and leads to *m/z* 141) competes effectively with propane loss (as opposed to what happens in Scheme 6). Moreover, the hydride transfer step gives an *m/z* 139 ion with a structure markedly different from the

**Scheme 8.** Reversible Proton Transfer within Ion–Neutral Complexes Leading to Butane Loss

*m/z* 139 in Scheme 6. HF loss can still take place (as shown), but it is not possible to expel a neutral ketone molecule upon CAD to give CF<sub>3</sub><sup>+</sup>, unless the neutral fragment has the zwitterionic structure drawn in Scheme 7 (or else corresponds to cyclopropanone). Similarly, this *m/z* 139 ion cannot easily access the four-membered cyclic transition state for metathesis, since that transition state would have to have the structure of a diradical (or else form a cyclopropane ring), as drawn. Hence, CF<sub>2</sub>O expulsion is barely detectable in the CAD of the *m/z* 139 from **22**, and CF<sub>3</sub><sup>+</sup> is not seen at all.

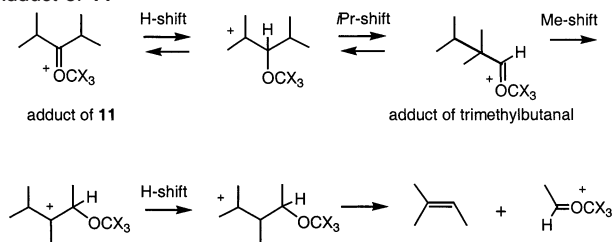
Ethyl ketones display a complex-mediated reaction that arises via a 1,2-hydride shift from the ethyl group, as Scheme 8 illustrates for the CF<sub>3</sub><sup>+</sup> adduct of 4-methyl-3-hexanone (**16**). The secondary cation that would result from the 1,2-shift has such an elongated C–C bond (calculated to have a bond length of 1.65 Å), that it might better be viewed as an ion–neutral complex containing a *sec*-butyl cation and 1-(trifluoromethoxy)propene, as drawn in Scheme 8. Hydride abstraction by *sec*-butyl cation<sup>22</sup> leads to expulsion of butane and formation of the CF<sub>3</sub><sup>+</sup> adduct of acrolein (*m/z* 125). Ketone **16** is the only one of the C<sub>7</sub>H<sub>14</sub>O ketones whose CF<sub>4</sub> CI gives an *m/z* 125 peak that is more intense than that of the *m/z* 139 (by a factor of 1.2). Ketone **22** also exhibits a significant *m/z* 125 ion, 0.6 the intensity of *m/z* 139, which must come from a complex containing a *tert*-butyl cation and 1-(trifluoromethoxy)propene.

The proton affinity of *trans*-1-(trifluoromethoxy)propene is calculated to be only 14 kJ mol<sup>-1</sup> greater than that of *trans*-2-butene. Reversible proton transfer between the partners in the ion–neutral complex from **16** takes place (as Scheme 8 depicts), which is revealed by a deuterium labeling experiment. For the α,α′-perdeuterated analogue (**16**-2,2,4-*d*<sub>3</sub>), two deuteria and two hydrogens undergo exchange, and the ions that result from butane loss are mono- (*m/z* 126) and dideuterated (*m/z* 127), in roughly a 4:3 ratio. One would predict that irreversible proton transfer followed by loss of monodeuterated butene should lead principally to a dideuterated ion, CH<sub>3</sub>CHDCD=OCF<sub>3</sub><sup>+</sup> (*m/z* 129). That peak has about half the intensity as *m/z* 127, while *m/z* 128 and 130 (mono- and trideuterated ions) together are >20 times more abundant (observed in roughly a 2:3 ratio).

Reversible proton transfer does not occur in the [(CH<sub>3</sub>)<sub>3</sub>C<sup>+</sup>CF<sub>3</sub>OCH=CHCH<sub>3</sub>] complex from **22**, since the proton affinity of isobutene is calculated to be 46 kJ mol<sup>-1</sup> greater than that of 1-(trifluoromethoxy)propene. Hydride abstraction by *tert*-butyl cation is calculated to be 18 kJ mol<sup>-1</sup> less endothermic than proton transfer. Since very little exchange takes place between the partners, the CF<sub>4</sub> CI of α,α′-perdeuterated **22** (**22**-2,2,4,4-

**Table 3.** Percentages of Major CF<sub>3</sub>-Containing Ions from Chemical Ionization of Isotopically Labeled Diisopropyl Ketones (**11a–c**) with CF<sub>4</sub> Reagent Gas in a Quadrupole Mass Spectrometer Using GC Sample Introduction

	MeCHO CF <sub>3</sub> <sup>+</sup>		Me <sub>2</sub> C=OCF <sub>3</sub> <sup>+</sup>	
	unlabeled ( <i>m/z</i> )	labeled ( <i>m/z</i> )	unlabeled ( <i>m/z</i> )	labeled ( <i>m/z</i> )
<b>11a</b> [(CH <sub>3</sub> ) <sub>2</sub> CH] <sub>2</sub> <sup>13</sup> CO	5 ( <i>m/z</i> 113)	73 ( <i>m/z</i> 114)	9 ( <i>m/z</i> 127)	5 ( <i>m/z</i> 128)
<b>11b</b> [CD <sub>3</sub> (CH <sub>3</sub> )CH] <sub>2</sub> CO	38 ( <i>m/z</i> 113)	36 ( <i>m/z</i> 116)	0.3 ( <i>m/z</i> 127)	12 ( <i>m/z</i> 130)
<b>11c</b> (CD <sub>3</sub> ) <sub>2</sub> CHCOCH(CH <sub>3</sub> ) <sub>2</sub>	38 ( <i>m/z</i> 113)	36 ( <i>m/z</i> 116)	5 ( <i>m/z</i> 127)	5 ( <i>m/z</i> 133) 4 ( <i>m/z</i> 130)

**Scheme 9.** Predominant Pathway for Rearrangement of the CF<sub>3</sub><sup>+</sup> Adduct of **11**

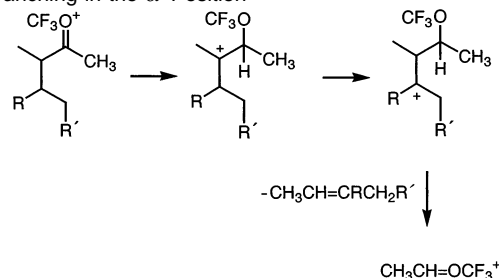
*d*<sub>4</sub>) gives the dideuterated ion (*m/z* 127 from hydride abstraction followed by C<sub>4</sub>H<sub>8</sub>D<sub>2</sub> loss) 10 times more often than the monodeuterated ion at *m/z* 126.

**Competing Decomposition Pathways.** When given the precedents of ketones **6** and **17**, the *m/z* 127 product ion from diisopropyl ketone, **11**, almost certainly must have the structure Me<sub>2</sub>C=OCF<sub>3</sub><sup>+</sup>. However, it is not easy from the mechanism in Scheme 2 to rationalize why MeCH=OCF<sub>3</sub><sup>+</sup> predominates over Me<sub>2</sub>C=OCF<sub>3</sub><sup>+</sup>, whose formation is thermochemically favored by >60 kJ mol<sup>-1</sup>. This evidence for kinetic control suggests an alternative pathway. The skeletal rearrangement mechanism exemplified by Scheme 9 can account for the result.

Alkyl shifts of this sort have precedent in acid-catalyzed rearrangements of branched ketones in solution.<sup>23</sup> For instance, the kinetics by which protonated **11** interconverts with protonated **12** have been measured in superacid solution.<sup>24</sup> As Scheme 9 depicts, a 1,2-hydrogen shift from the position adjacent to the carbonyl in the adduct forms a tertiary carbocation. A 1,2-shift of the alkyl group on the other side of the carbonyl then gives a rearranged oxygen-stabilized cation. Another 1,2-alkyl shift produces a rearranged carbocation, in which a subsequent 1,2-shift yields a carbocation from which alkene may easily be lost.

To distinguish the oxygen transposition pathway shown in Scheme 2 from the alkyl shift mechanism in Scheme 9, we have prepared diisopropyl ketone with <sup>13</sup>C at the carbonyl carbon, compound **11a**. Scheme 9 predicts that the label should remain with the ionic product. If oxygen transposition were to take place, the <sup>13</sup>C should be lost in the expelled neutral. The data summarized in Table 3 show that alkyl shift (Scheme 9) predominates over oxygen migration by a factor of 6.5:1. In the MeCHO CF<sub>3</sub><sup>+</sup> product ion, the ratio of <sup>13</sup>C-containing to unlabeled ions is 14.5:1. The ratio of labeled to unlabeled ions in the Me<sub>2</sub>C=OCF<sub>3</sub><sup>+</sup> product ions is 1:1.8.

The foregoing discussion explains why **17**, **18**, and **22** are the only C<sub>7</sub>H<sub>14</sub>O ketones that yield more *m/z* 127 than *m/z* 113. As discussed above, the CF<sub>3</sub><sup>+</sup> adduct of **22** undergoes a 1,3-

**Scheme 10.** Alkene Loss from Adduct Ions of Methyl Ketones with Branching in the α'-Position

hydrogen shift (Scheme 4) to about the same extent as it undergoes the sequence of successive 1,2-shifts depicted in Scheme 5 (R = H, R' = Me). Compounds **17** and **18** are the sole isomers without α-hydrogens on both sides of the carbonyl. The similarity of the product distributions from **17** and **18** suggests that their CF<sub>3</sub><sup>+</sup> adducts interconvert extensively via 1,2-alkyl shifts (as protonated **17** and **18** do in solution<sup>25</sup>). Similarly, the C<sub>6</sub>H<sub>12</sub>O ketones **6** and **7** give the same product distributions, implying that their adducts equilibrate before decomposition (as protonated **6** and **7** are reported to do in the gas phase,<sup>26</sup> as well as in solution<sup>25</sup>).

There is no evidence that branching in the β-position alters the rearrangement chemistry when the first 1,2-shift can form a tertiary carbocation center. Scheme 10 displays a sequence of 1,2-hydrogen shifts that corresponds to the major decomposition pathway for the adduct of **12** (R = Me, R' = H). CF<sub>4</sub> chemical ionization of compound **14** (R = H, R' = Me), which has no β-branching, yields virtually the same distribution of ion products as does that of **12**.

As in the case of **6** and **17**, methyl deuteration exerts a negligible effect on the product distribution. The proportions of labeled MeCHO CF<sub>3</sub><sup>+</sup> are virtually the same for the two isomeric β,β-*d*<sub>6</sub> ketones **11b** and **c**. This might conceivably reflect randomization of all four methyl groups, but the differences among the labeled Me<sub>2</sub>C=OCF<sub>3</sub><sup>+</sup> ions argue against that possibility (for which naïve statistics would predict a 1:4:1 ratio of *m/z* 127:130:133). It is more likely that the small isotope effect is a consequence of the reversibility of the *i*Pr-shift in Scheme 9. The reversibility of this step and of the antecedent 1,2-hydride shift explains why MeCHO CF<sub>3</sub><sup>+</sup> prevails even in ketones such as 4-heptanone (**10**), where reiterated 1,2-shifts must be invoked.

The predominance of C<sub>3</sub>H<sub>6</sub>OCF<sub>3</sub><sup>+</sup> ions in **17** and **18** suggests that an even higher degree of branching should further suppress MeCHO CF<sub>3</sub><sup>+</sup> production. As the result for pentamethylacetone (*tert*-butyl isopropyl ketone, **25**) indicates, such is the case. In

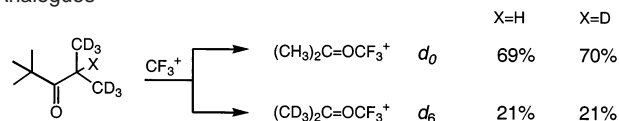
(23) Oka, M.; Hinton, J.; Fry, A.; Whaley, T. W. *J. Org. Chem.* **1979**, *44*, 3545–3550.

(24) Brouwer, D. M.; van Doorn, J. A. *Recl. Trav. Chim. Pays-Bas* **1971**, *90*, 535–548.

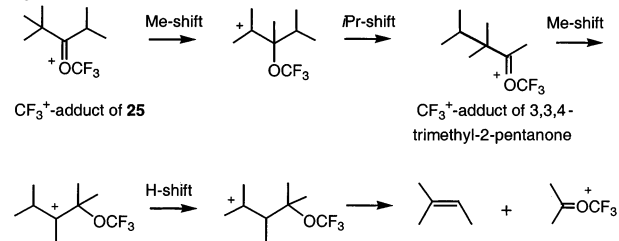
(25) Brouwer, D. M.; van Doorn, J. A. *Recl. Trav. Chim. Pays-Bas* **1971**, *90*, 1010–1026.

(26) Weiss, M.; Crombie, R. A.; Harrison, A. G. *Org. Mass Spectrom.* **1987**, *22*, 216–223.

**Scheme 11.**  $\text{CF}_3^+$  Adduct of Acetone is Virtually the Only Product Ion from  $\text{CF}_4/\text{Cl}$  of Pentamethylacetone (**25**) and Its Deuterated Analogues



**Scheme 12.** Predominant Pathway for Rearrangement of the  $\text{CF}_3^+$  Adduct of **25**



the FT-ICR spectra,  $\text{Me}_2\text{C}=\text{OCF}_3^+$  is the major product from the reaction of **25** with  $\text{CF}_3^+$ . That peak is about twice as intense as that of the next most abundant ion–molecule reaction product, isopropyl cation, and virtually no  $\text{MeCH}=\text{OCF}_3^+$  is seen. Similarly,  $\text{Me}_2\text{C}=\text{OCF}_3^+$  constitutes >90% of the fluorine-containing ions from  $\text{CF}_4$  chemical ionization in the sector and quadrupole mass spectrometers. The deuterium labeling experiments summarized in Scheme 11 (where the percentages represent fractions of the total ion yield from  $\text{CF}_4$  chemical ionization and the  $d_3$  ion constitutes <5% of the product) indicate that methyl shift is more probable than hydride shift as the initial step in the rearrangement.

Scheme 12 illustrates how an initial methyl shift would produce the  $\text{CF}_3^+$  adduct of acetone via expulsion of 2-methyl-2-butene, by direct analogy to Scheme 9. However, the same labeling result would have been obtained if an oxygen migration (cf. Scheme 2 with R = methyl) had occurred instead. The known rearrangement of **25** to 3,3,4-trimethyl-2-pentanone in sulfuric acid<sup>17</sup> proceeds via alkyl shift. On the basis of that precedent (and on the results for the  $^{13}\text{C}$ -labeled diisopropyl ketone **11a**), it seems reasonable to infer that Scheme 12 operates in preference to Scheme 2.

## Discussion

The data presented here provide evidence that the addition of Lewis superacidic ions to a carbonyl oxygen can induce skeletal rearrangements on the sub-microsecond time scale. Out of the 24 saturated  $\text{C}_5$ – $\text{C}_7$  ketones, 10 do not have a methyl group attached directly to the carbonyl carbon. Nevertheless, 8 of those 10 (such as 3-pentanone) exhibit  $\text{MeCH}=\text{OCF}_3^+$  as the most abundant ion–molecule reaction product with  $\text{CF}_3^+$ . An isotopic labeling experiment shows that this comes about as a result of at least two alkyl shifts, in addition to hydrogen shifts.

Electrophiles stronger than anhydrous aluminum trichloride have been called Lewis superacids.<sup>27</sup> By that criterion, most  $sp^2$ -hybridized organic cations are Lewis superacids. As Table 4 summarizes, the calculated binding energies of representative cations to water, formaldehyde, and acetone<sup>28</sup> are substantially greater than those of aluminum trichloride. Also, while the cations add to acetone much more exothermically than to water,

**Table 4.** Density Functional Theory (B3LYP/6-311G\*\*) Binding Energies of Oxygen Nucleophiles to Representative Cations (from ref 28) and to Aluminum Trichloride (in  $\text{kJ mol}^{-1}$ )

	$\text{H}_2\text{O}$	$\text{CH}_2=\text{O}$	$(\text{CH}_3)_2\text{C}=\text{O}$
$\text{CH}_3^+a$	320	336	411
$\text{CF}_3^+a$	182	199	291
$\text{Me}_3\text{Si}^+a$	166	157	207
$\text{AlCl}_3^+b$	128	106	133
BSSE	23	14	15
$\Delta\text{ZPE}$	9	9	6
$\Delta H_{\text{dissn}}$	96	83	112

<sup>a</sup> As reported in ref 28, without zero point energy ( $\Delta\text{ZPE}$ ) or basis set superposition error (BSSE) corrections. <sup>b</sup> This work.

aluminum trichloride has an affinity for acetone that is a mere  $16 \text{ kJ mol}^{-1}$  greater than its affinity for water.

When  $\text{CF}_3^+$  acts as the electrophile, halonium metathesis can compete with rearrangement. Yet, in nearly all of the cases studied, rearrangement wins out over metathesis. This provides a different perspective from what is learned by studying protonated,<sup>26</sup> methylated, or trimethylsilylated<sup>19,20</sup> species, since there is no low-barrier alternative to isomerizations of these latter ions. The barrier for metathesis provides an upper bound for the barrier to rearrangement.

The study of  $\text{CF}_3^+$  adducts answers questions that have not been addressed by previous experiments.  $\text{CF}_3^+$  adducts exhibit analogies to reactions seen in strongly acidic solutions,<sup>23–25</sup> but on a time scale that is a factor of  $10^9$  shorter. While the metastable ion decompositions of protonated ketones<sup>26</sup> also hint at a rich rearrangement chemistry, the dominant reaction (water loss) does not allow an assessment of whether it is the carbon skeleton that isomerizes. Nor is there a competing reaction that permits a systematic study of the features that enhance or inhibit rearrangement.

Previous ion–molecule studies of gaseous Lewis superacids display products that cannot be explained in terms of simple disconnections of the parent structure, such as the formation of  $\text{C}_3\text{H}_6\text{OB}(\text{OMe})_2^+$  and a trace of  $\text{CH}_3\text{CH}=\text{OB}(\text{OMe})_2^+$  from the reaction of  $(\text{MeO})_2\text{B}^+$  with 4-heptanone.<sup>29</sup> In a similar vein, we have recently reported a systematic study of the gaseous adducts of trimethylsilyl cation ( $\text{TMS}^+$ ) with saturated ketones,<sup>20</sup> whose metastable ion decompositions parallel the isomerizations of protonated ketones that have been observed in solution.<sup>24,25</sup> In these examples, however, the question of whether the transpositions seen in the gas-phase result from oxygen migration or alkyl shift has been left unresolved.

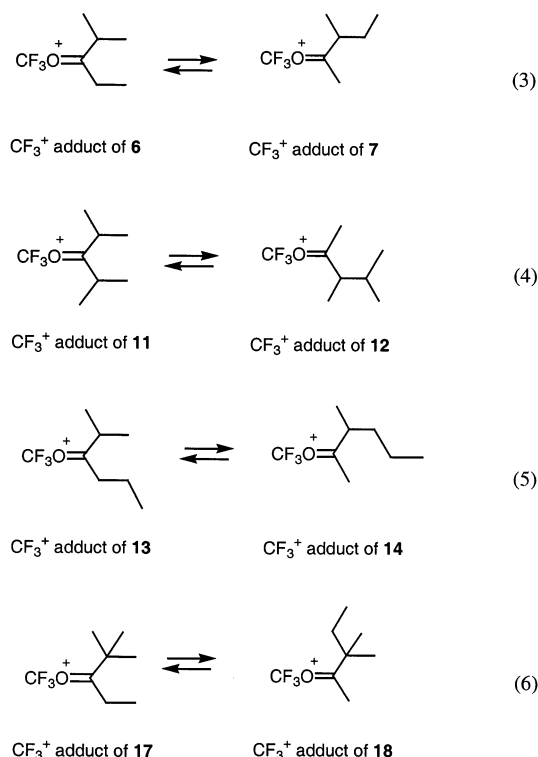
The present study resolves this question in favor of alkyl shift.  $\text{CF}_3^+$  attacks diisopropyl ketone to give  $\text{MeCH}=\text{OCF}_3^+$  as nearly three-quarters of the total ion yield. The labeling result for **11a** (summarized in Table 3) shows that the  $^{13}\text{C}$ -tagged carbonyl carbon stays connected to oxygen 94% of the time. Equations 3–6 illustrate the results of alkyl shift for four pairs of ketones that ought to equilibrate via this mechanism. Our experiments show that this prediction is borne out, as can be inferred from Table 1. As noted above, all of the ketones studied exhibit distinctive  $\text{CF}_4$  CI patterns, except for those whose  $\text{CF}_3^+$  adducts are shown in eqs 3–6.

The experiments reported here provide strong evidence for the generality of alkyl shifts that make and break more than one carbon–carbon bond. Transposition of alkyl groups from

(27) Olah, G. A.; Surya Prakash, G. K.; Sommer, J. *Science* **1979**, *206*, 13–19.  
 (28) Basch, H.; Hoz, T.; Hoz, S. *J. Phys. Chem. A* **1999**, *103*, 6458–6467.

(29) Ramatunga, T. D.; Kennady, J. M.; Kenttämaa, H. I. *J. Am. Chem. Soc.* **1997**, *119*, 5200–5207.





one side of the carbonyl to the other can take place via the mechanism shown in Scheme 9. The CF<sub>3</sub><sup>+</sup> adducts of **6** and **7** transpose a methyl and an ethyl, as do the adducts of **17** and **18**. The CF<sub>3</sub><sup>+</sup> adducts of **13** and **14** transpose a methyl and a propyl, while the adducts of **11** and **12** transpose a methyl and an isopropyl. These isomerizations proceed to a sufficient extent that the above pairs of ketones give the same CF<sub>4</sub> CI patterns. Moreover, these skeletal rearrangements (and the consequent expulsion of neutral hydrocarbons) prevail, for the most part, over metathesis.

Competition between halonium metathesis and isomerization of the CF<sub>3</sub><sup>+</sup> adduct of **11** has been examined by DFT calculations on the relevant transition states. Figure 1 portrays four pathways. The adduct of **11** is placed in the center of the figure. Rotation about the carbon–oxygen bond (represented by the dashed curve) is required for metathesis. This rotation has a comparatively low barrier. The two highest rearrangement barriers are drawn to the left in Figure 1. The four-membered ring corresponding to metathesis lies much higher than any of the other transition states. The transition state for forming an [iPr<sup>+</sup> C<sub>4</sub>H<sub>7</sub>OCF<sub>3</sub>] ion–neutral complex via methyl shift has virtually the same energy as that of the complex itself and is 70 kJ mol<sup>-1</sup> lower in energy than that of the metathesis transition state. Hydride shift to form a tertiary alkyl cation, the curve to the right, has an even lower barrier. The two pathways leading from that intermediate, isopropyl shift versus CF<sub>3</sub>O-migration, differ in energy by 25 kJ mol<sup>-1</sup>. The CF<sub>3</sub>O-migration passes through a three-membered cyclic transition state and has the higher barrier. Isopropyl shift leads to the CF<sub>3</sub><sup>+</sup> adduct of 2,2,3-trimethylbutanal, as Scheme 9 portrays. DFT geometry optimization predicts an unusually long bond length between the two tertiary carbons in that aldehyde adduct, and it is more appropriately viewed as an ion–neutral complex, as drawn to the right in Figure 1. This structure, therefore, offers a second

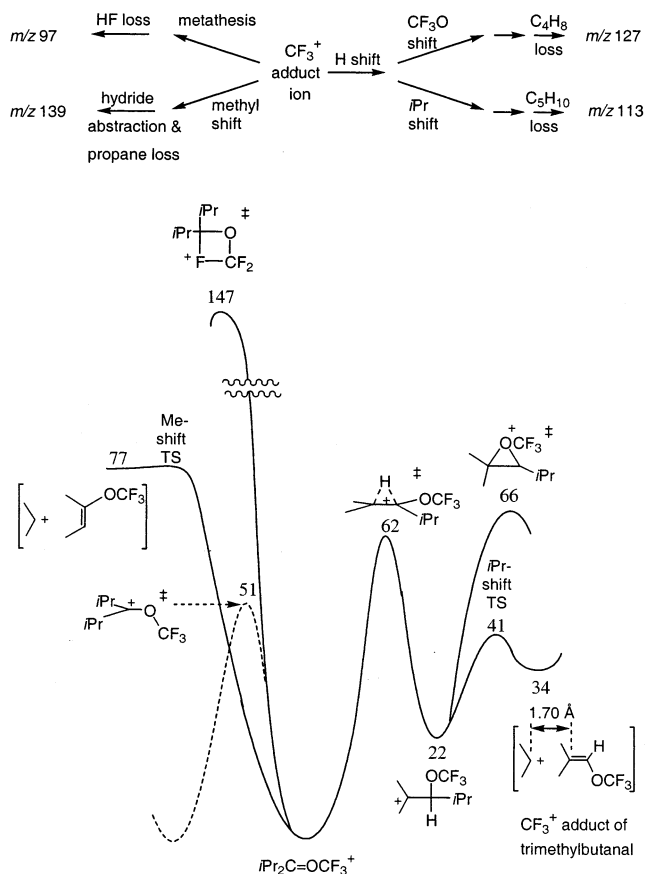


**Figure 1.** DFT calculated intermediates and transition states (energies given in kJ mol<sup>-1</sup>) for the reaction of diisopropyl ketone (**11**) with CF<sub>3</sub><sup>+</sup>, showing the branching among competing pathways. The CF<sub>3</sub><sup>+</sup> adduct of **11** (corresponding to the lowest well) is initially formed with an internal energy approximately 125 kJ mol<sup>-1</sup> higher than that of the barrier for metathesis (corresponding to the highest transition state).

available pathway to propane expulsion, as well as being an intermediate for the interconversion in eq 3.

The product ratio from CF<sub>4</sub> CI of **11** agrees qualitatively with the DFT energetic ordering of barrier heights: *m/z* 97:127:139:113 are seen in a ratio of 1:2:2:18 (when the experimental proportions of alkene loss are corrected on the basis of the <sup>13</sup>C labeling results for **11a** in Table 3). The fact that metathesis is observed at all (albeit with subsequent loss of HF), despite having a barrier of 85 kJ mol<sup>-1</sup> higher than C<sub>5</sub>H<sub>10</sub> expulsion, reflects the high vibrational energy content of initially formed CF<sub>3</sub><sup>+</sup> adducts. When attachment occurs at low pressures (as in an FT-ICR instrument), or if ions are extracted from the source region faster than the rate of collisions with neutral gas molecules, the distribution of reaction products reflects the pathways chosen by chemically activated adduct ions.

Under the CI conditions reported here, no more than a few percent of the initially formed CF<sub>3</sub><sup>+</sup> ions react with neutral ketones in the ion source, since the ion–molecule collision rate is ≤10<sup>4</sup> per second, approximately 2 orders of magnitude slower than the rate with which they are extracted from the source. Thus, the unimolecular rearrangements described here represent the decompositions of chemically activated species whose internal energy is approximately equal to the exothermicity of the initial addition step. It is, therefore, interesting to note that the interconversions in eqs 3–6 (or, at least, the decompositions of those adduct ions through sets of common intermediates)

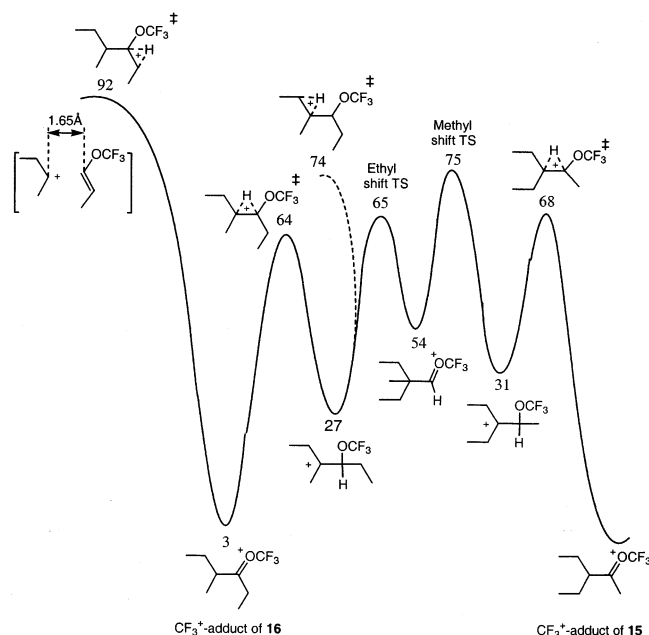
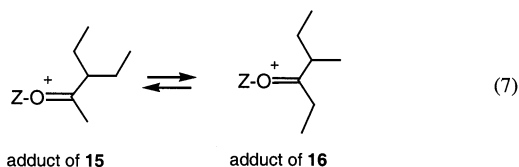


**Figure 2.** DFT calculated intermediates and transition states for interconversion of the  $\text{CF}_3^+$  adducts of **15** and **16** in competition with dissociation pathways (energies given in  $\text{kJ mol}^{-1}$ ). The  $\text{CF}_3^+$  adducts are initially formed with internal energies approximately  $180 \text{ kJ mol}^{-1}$  greater than that of the highest transition state.

have gone virtually to completion prior to fragmentation. Evidence of this has also been seen in metastable ion decompositions of  $\text{TMS}^+$  adducts.<sup>19,20</sup> The present results demonstrate that such rearrangements can take place on a shorter time scale.

The mechanism in Scheme 9 predicts that five pairs of isomeric  $\text{CF}_3^+$  adducts ought to interconvert: namely, those shown in eqs 3–7. The  $\text{TMS}^+$  adducts of all five pairs do exhibit this sort of isomerization (including eq 7, where  $Z = \text{trimethylsilyl}$ ), but the  $\text{CF}_4$  CIs of **15** and **16** display markedly different patterns. In this case, the rate of interconversion must be slower



than that of decomposition. To probe that issue more closely, the DFT calculations in Figure 2 compare the intermediates and transition states for butane and butene loss from the  $\text{CF}_3^+$  adduct of **16** with its isomerization to the  $\text{CF}_3^+$  adduct of **15**. By analogy to Scheme 9, the isomerization should pass through three intermediates: a tertiary cation, the  $\text{CF}_3^+$  adduct of an aldehyde, and another tertiary cation (as Figure 2 depicts) en route to the  $\text{CF}_3^+$  adduct of **15** (drawn to the far right). The first tertiary cation can lose 2-butene to give the  $\text{CF}_3^+$  adduct of propionaldehyde ( $m/z$  127, the most abundant ion from **16**), as represented by the dashed curve. The second tertiary cation can lose 2-pentene to give the  $\text{CF}_3^+$  adduct of acetaldehyde ( $m/z$  113, the next most abundant ion). Experimentally,  $\text{CF}_4$  CI of

**15** gives more  $m/z$  113 than  $m/z$  127, in line with the calculated energy profile. Butane loss (Scheme 8) takes place via the ion–neutral complex drawn to the far left, whose heat of formation is nearly the same as that of the hydride-shift transition state that leads to it.

Figure 2 contains four hydride-shift transition states. The two that are involved in eq 7 ( $Z = \text{CF}_3$ ) are lower than the other two. The barrier for the hydride shift leading ultimately to the elimination of butane (at the far left, corresponding to Scheme 8) is higher than the one leading to the expulsion of *cis*-2-butene (dashed curve). The [*cis*-2-butene  $\text{EtCH}=\text{OCF}_3^+$ ] complex that forms from the hydride shift lies  $2 \text{ kJ mol}^{-1}$  lower than the transition state. The barrier is lower than the barrier for the competing methyl shift, which is a necessary step in eq 7. Thus, DFT calculations provide a rationalization as to why eq 7 (unlike eq 3) does not go much faster than butene expulsion.

Curiously, the electronic energy and zero point energy of the transition state for the expulsion of *trans*-2-butene are higher than those for the *cis*. When counterpoise is used to estimate the basis set superposition errors for both the *cis* and *trans* transition states, the net barrier height difference is  $6.5 \text{ kJ mol}^{-1}$  in favor of *cis*-2-butene elimination. If the DFT calculations are correct, they predict a contrathermodynamic distribution of geometrical isomers of 2-butene.

## Conclusions

The methyl cation and  $\text{CF}_3^+$  are Lewis superacids.  $\text{CF}_3^+$  is not as strong a Lewis acid as methyl cation, but it has a much greater propensity to undergo halonium metathesis. Nevertheless, methyl cation and  $\text{CF}_3^+$  both react with ketones at low pressures to yield product ions that correspond to rearrangements of the carbon skeleton. Within a few microseconds, the vibrationally excited adduct ions undergo multiple alkyl shifts, which are analogous to slower transpositions seen for protonated ketones in solution. The resulting deep-seated rearrangements compete favorably not only with halonium metathesis but also with prompt fragmentations that require only hydride shifts. The same sorts of rearrangements take place within Lewis superacid adducts in the gas phase, as have been observed for protonated ketones in solution on a time scale that is a factor of  $10^9$  longer.

An adduct ion does not have to have very many carbons in order for quite elaborate mechanisms to dominate its chemistry. Scheme 1 illustrates a case in point, where the series of skeletal rearrangements summarized in Scheme 9 has been shown to take place. This reaction occurs with both methyl and  $\text{CF}_3^+$  adducts. Of the 25 ketones studied here, all but 8 give the same product,  $\text{CH}_3\text{CH}=\text{OCF}_3^+$ , even though that ion is not the most favorable thermodynamic outcome. DFT calculations account for the kinetic control in terms of relative barrier heights for competing isomerizations. The observed rearrangements produce trifluoromethylated ions that are otherwise difficult to prepare. This chemistry is the subject of continuing investigation.

**Acknowledgment.** The authors are grateful to Dean Phillips for preparing pentamethylacetone. This work was supported by NSF Grant CHE 9983610 and by the CNRS.

JA020557+